THE JOURNAL OF PHYSICAL CHEMISTRY B

Article

pubs.acs.org/JPCB

Water's Structure around Hydrophobic Solutes and the Iceberg Model

N. Galamba*

Grupo de Física-Matemática, Universidade de Lisboa, Avenida Prof. Gama Pinto 2, 1649-003 Lisboa, Portugal

ABSTRACT: The structure of water in the hydration shells of small hydrophobic solutes was investigated through molecular dynamics. The results show that a subset of water molecules in the first hydration shell of a nonpolar solute have a significantly enhanced tetrahedrality and a slightly larger number of hydrogen bonds, relative to the molecules in water at room temperature, consistent with the experimentally observed negative excess entropy and increased heat capacity of hydrophobic solutions at room temperature. This ordering results from the rearrangement of a small number of water molecules near the nonpolar solutes that occupy one to two vertices of the enhanced water tetrahedra. Although this structuring is not nearly like that often associated with a literal interpretation of the term "iceberg" in the Frank and Evans iceberg model, it does support a moderate interpretation of this model. Thus, the tetrahedral orientational order of this ensemble of water molecules is comparable to that of liquid water at ~10 °C, although not accompanied by the small contraction of the O−O distance observed in cold water. Further, we show that the structural changes of water in the vicinity of small nonpolar solutes *cannot* be inferred from the water radial distribution functions, explaining why this increased ordering is not observed through neutron diffraction experiments. The present results restore a molecular view where the slower translational and reorientational dynamics of water near hydrophobic groups has a structural equivalent resembling water at low temperatures.

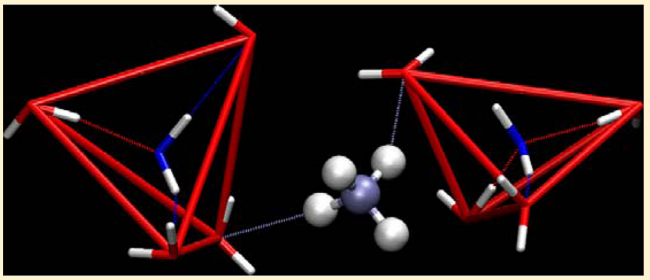

INTRODUCTION

The hydration and interaction of hydrophobic groups and molecules play key roles in several chemical and biological processes.[1−3] Examples include membrane assembly and protein folding, where hydrophobic groups aggregate to "hide" from water.[2,4,5] The low solubility of nonpolar molecules at room temperature is characterized by a small decrease of the standard enthalpy, $\Delta^{\circ}H$, and a large decrease of the standard entropy, $\Delta^{\circ}S$, upon transfer to water, resulting in a large positive standard Gibbs energy, $\Delta^{\circ}G$.[1,4,5] Furthermore, the hydration of hydrophobic solutes is accompanied by an increase of the heat capacity, C_p, also observed upon protein denaturation.[1,6] This increase in C_p and the low negative $\Delta^{\circ}H$ and large negative $\Delta^{\circ}S$ suggest that water molecules are more ordered around nonpolar molecules and groups than in pure water at the same temperature and pressure. In 1945, Frank and Evans[7] proposed the so-called iceberg model to explain the thermodynamics of hydration of hydrophobic solutes. According to this model, a subset of water molecules, those nearest the solute, should have an "icelike" structure, forming a pseudocrystalline cage around the hydrophobe, explaining the $\Delta^{\circ}H$, $\Delta^{\circ}S$, and C_p values that characterize the transfer of nonpolar solutes to water. Further, it has been proposed that the cavity containing a small solute molecule could consist of pentagonal rings, similar to those found in natural gas hydrates, rather than hexagonal rings of ice.[2] However, this view has been contradicted by theoretical[8] and simulation studies.[9] Even though the iceberg model is appealing in that it provides a plausible explanation for the large entropy decrease and heat capacity increase, it lacks experimental, theoretical, and molecular simulation support.[1,2] Thus, instead, water molecules around small hydrophobic solutes are thought to orient with at least one O−H bond tangential to the solute surface without noticeable H-bonding enhancement. The interpretation of neutron diffraction results for a solution of methane in water at 18 °C and 180 bar, for instance, suggested that, if anything, the structure of water is marginally *less* tetrahedral than that of pure water at the same temperature and pressure.[10] A vibrational sum frequency study[11] also indicated weak hydrogen bonding between water molecules, although at hydrophobic surfaces where hydrophobic hydration is distinct from the hydration of small nonpolar solutes.[3,12,13] A Monte Carlo study on the hydration of methane at 320 K and different pressures showed that hydration-shell water molecules have a smaller number of H-bonds, a smaller number of near neighbors, and a lower tetrahedrality than bulk water molecules.[14] This lack of experimental support for the iceberg model has led to the proposal of alternative models and theories to account for the thermodynamics of hydration of nonpolar molecules and groups.[2,6,12,13,15−27]

The entropy decrease upon the transfer of hydrophobic solutes to water is also commonly interpreted in terms of the slower dynamics of water in the solute's hydration shell, observed experimentally[28−37] and through molecular simula-

Received: October 27, 2012
Revised: December 29, 2012
Published: January 29, 2013

tions.[38−43] Nevertheless, the extent of this slowdown is also controversial. The orientational dynamics of water was studied by femtosecond midinfrared[30] and two-dimensional infrared (IR) spectroscopy,[44] indicating that some water molecules are immobilized around hydrophobic groups. This observation is not supported by most molecular dynamics[38−42] or nuclear magnetic resonance[29,31,33,34,36,37] studies, which predict a moderate slowdown of the reorientational dynamics of water. A recent molecular dynamics (MD) study,[45] however, found a slowdown of some water molecules near a hydrophobic molecule similar to that found by Rezus and Bakker through femtosecond midinfrared spectroscopy.[30] These results are therefore consistent with the iceberg model although from a dynamical viewpoint. Thus, the current view on hydrophobic hydration is that water molecules near nonpolar groups have slower translational and reorientational dynamics, even though the structure of water remains nearly unperturbed relative to that of bulk or pure water. It should be expected, however, that a moderate or significant loss of translational and rotational freedom of water would have a structural equivalent similar, to some extent, to water at low temperatures. Following the discussion by Southall et al.[6] on Kauzmann's[4] interpretation of the iceberg model, even though water around nonpolar solutes should be *less ordered* and *different than ice*, experimental determination of the amount of water structuring in the hydration shells remains elusive. Here, we show that this structural equivalent exists, although it is not like that suggested from a literal interpretation of the iceberg term in the iceberg model of Frank and Evans. Thus, instead, we find a milder ordering of water more similar to the aforementioned molecular picture foreseen by Kauzmann. Further, we anticipate that, unlike liquid water at low temperatures, a small contraction of the O−O distance of water is not observed near the solute and that the water partial radial distribution functions in the hydrophobic aqueous solutions are indistinguishable from those of neat water, consistent with neutron diffraction results.[10,46] We carried out MD of aqueous solutions of four small hydrophobic molecules of different sizes and shapes, specifically, xenon, methane, ethane, and benzene, described by the flexible and polarizable model AMOEBA.

METHODS

Molecular dynamics (MD) simulations of aqueous solutions of a single atom of xenon, or of a single molecule of methane, ethane, or benzene, and 256 water molecules at 298.15 K and 1 atm were carried out with the flexible and polarizable force field AMOEBA 04.[47,48] MD results for pure water at 283.15 and 298.15 K are also reported for comparison purposes. The MD simulations were performed with the program TINKER 5.1.[49] The long-range electrostatic interactions were calculated with the Ewald sum and the particle mesh Ewald method as implemented in TINKER. Nonbonded van der Waals interactions and the Ewald real-space summation were truncated at $L/2$, where L is the average length of the cubic MD box after equilibration. A modified Beeman algorithm was used to integrate the equations of motion with a time step of 0.5 fs. The systems were equilibrated for 150 ps in the (N,V,T), isokinetic environment, followed by an (N,P,T) simulation for 300 ps at the same temperature and 1 atm, using the thermostat and barostat of Berendsen et al.[50] For water at 283 K, an additional 500 ps of simulation was performed at (N,P,T) conditions for equilibration purposes. The production runs were carried out for 1.0 ns through (N,P,T) MD for every system. The average volumes for the distinct hydrophobic solutions were similar, corresponding to a concentration of ∼0.2 M. Further, MD in the microcanonical ensemble for neat water and for xenon and methane solutions at the average volumes of the respective (N,P,T) simulations were carried out for comparison purposes, in particular, to probe the effect of Berendsen et al.'s thermostat and barostat on the water structure, as these techniques do not generate the exact (N,P,T) ensemble.

RESULTS AND DISCUSSION

Hydration and H-Bonding. We probed the structure of water in the regions R_n (n = 1, 2, 3, 4) defined by the maxima and minima of the first and second peaks (see Figure 1) of the

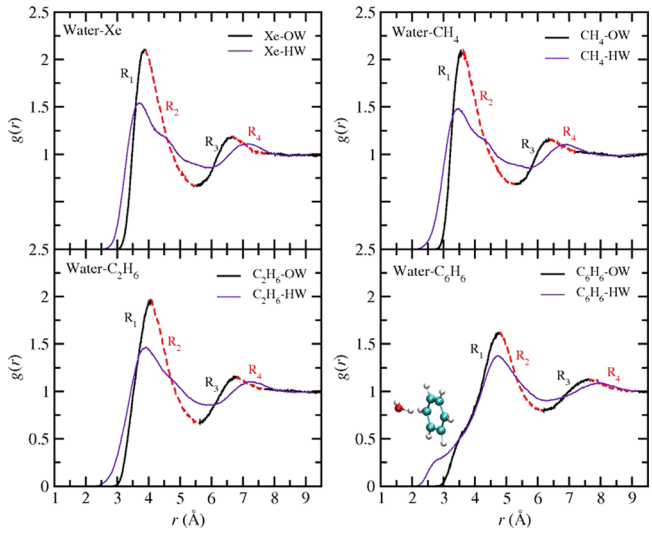

Figure 1. s−OW and s−HW (s = Xe, CH_4, C_2H_6, and C_6H_6) radial distribution functions (RDFs) and the four distinct regions defined by the respective maxima and minima of the s−OW RDF. The hydrocarbon−water RDFs were computed for the centers of mass of the solutes. The numbers of water molecules (O atoms) in R_1, R_2, R_3, and R_4, respectively, were as follows: Xe (4.7, 21.4, 37.5, and 66.7), CH_4 (3.8, 18.9, 33.6, and 50.2), C_2H_6 (6.4, 22.3, 40.1, and 61.4), and C_6H_6 (10.7, 29.1, 57.7, and 100.9). The shoulder at $r \approx 3.0$ Å of the C_6H_6−HW pair function corresponds to the single aromatic $\pi\cdots$HW H-bond (N_H = 1).

s−OW (s = Xe, CH_4, C_2H_6, C_6H_6) radial distribution functions (RDFs). This distinction, in particular, the separation of the first hydration shell in regions R_1 and R_2, was motivated by the fact that water molecules in R_1 are not always at the center of a water tetrahedron and, therefore, have a lower number of water−water H-bonds. Figure 2 shows the numbers of water−water donor and acceptor H-bonds for the distinct regions and solutes. The number of H-bonds was calculated using the following geometric criteria: $r_{OO} < 3.3$ Å and $\phi_{HOO} < 30°$, where r_{OO} is the distance between the donor and acceptor oxygen atoms and ϕ_{HOO} is the angle between the intramolecular O−H bond and r_{OO}. For the hydrocarbons, but not for Xe, water can form weak H-bonds[51] with the solute, as either a proton donor or a proton acceptor. The fact that the number of water−water acceptor H-bonds in R_1 was slightly lower than the number of donors could, perhaps, be interpreted in terms of the suggested[52] preferential role of hydrocarbons in solution as proton donors, opposite to the case for the gas phase. Nonetheless, this difference was most significant for

dx.doi.org/10.1021/jp310649n | J. Phys. Chem. B 2013, 117, 2153−2159

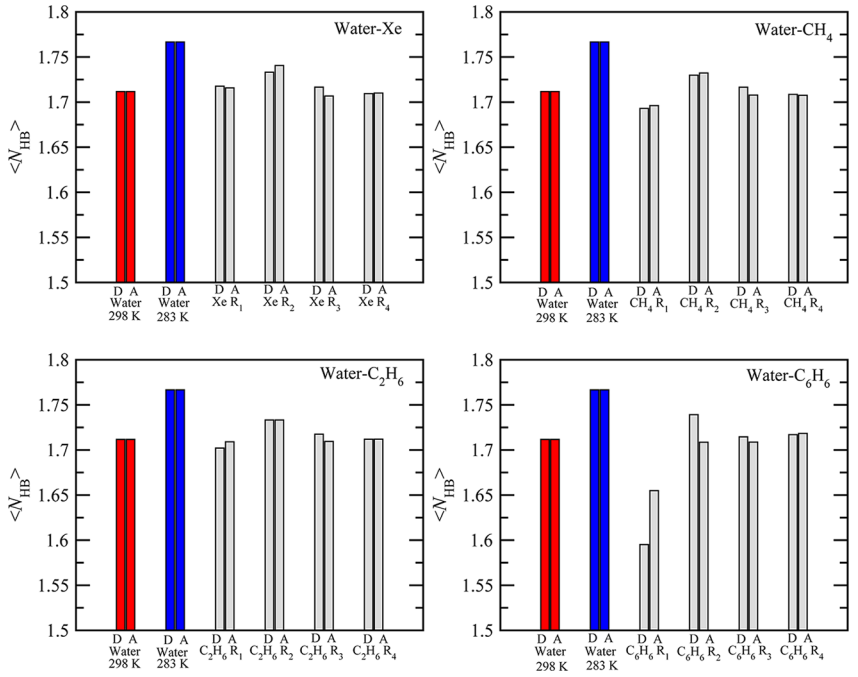

Figure 2. Average numbers of donor (D) and acceptor (A) H-bonds in neat water at 298 and 283 K and in the distinct regions R_1–R_4 around hydrophobic solutes.

benzene, and the numbers of H-bonds observed in R_1 for the methane and ethane solutions were consistent with the view that water molecules are oriented (on average) with at least one O–H bond tangential to the solute, without significant H-bond breaking (or enhancement) relative to that in pure water at the same temperature and pressure. This reflects the fact that water–water interactions are dominant relative to solute–water interactions, and therefore, the ability of methane and ethane to orient the surrounding waters is relatively weak. Benzene is different from aliphatic hydrocarbons in that it forms a single WH$\cdots\pi$ H-bond[53−56] in addition to possible weak H-bonds involving benzene's C and H atoms. This aromatic WH$\cdots\pi$ H-bond corresponds to the shoulder at ∼3.0 Å in the C_6H_6–HW RDF (see Figure 1). An MD study[55] on the hydration of benzene with the AMOEBA potential showed that this force field, unlike nonpolarizable potentials, gives a description of the water structure on the equatorial and axial regions of benzene similar to that obtained from first-principles MD.[53] The number of H-bonds in R_2 is larger for both Xe and the hydrocarbons, whereas in the second hydration shell (R_3 and R_4), the number of H-bonds is nearly equal to the number in pure water. The increase in the number of H-bonds in R_2 is, however, significantly smaller than that observed for neat water at 283 K (N_{HB} = 3.54), plotted here for comparison purposes. Furthermore, if one considers the average number of H-bonds in the first hydration shell (R_1 and R_2), no significant enhancement or disruption was found, relative to that in neat and bulk water, especially for methane and ethane.

Water Tetrahedrality. The tetrahedrality of the H-bond network of water was probed with recourse to the orientational order parameter, q, proposed by Chau and Hardwick,[57] but in the rescaled version introduced by Errington and Debenedetti.[58] This parameter is given by $q = 1 - {}^3/_8 \sum_{i=1}^{3} \sum_{j=i+1}^{4} (\cos \theta_{ij} + {}^1/_3)^2$, where θ_{ij} is the angle formed by the lines joining the O atom of a given water molecule and those of its nearest neighbors, i and j ($\leq$4); the average value of q varies between 0 (ideal gas) and 1 (perfect tetrahedral H-bond network). The distributions of the tetrahedral parameter, q, for pure water at 298 and 283 K, and for the distinct solutions are given in Figure 3. A significant enhancement of the tetrahedral orientational

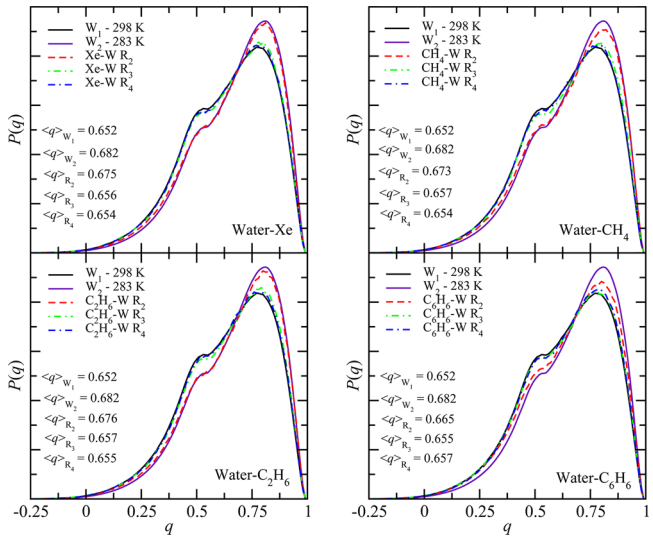

Figure 3. Distribution of the tetrahedrality parameter, q, in neat water and in regions R_2–R_4 around hydrophobic solutes.

order is observed in R_2, relative to that observed in neat water at 298 K, whereas outside the first hydration shell (R_3 and R_4), water tetrahedrality is much more similar to the orientational order found in neat water. The average value of q in R_2 was similar for xenon, methane, and ethane and lower for benzene. A slightly larger tetrahedral enhancement was previously reported[55] for benzene, from an MD simulation at constant (N,V,T); this difference should be related to pressure differences between the simulations. Thus, it can be seen from Figure 3 that, especially for Xe, CH_4, and C_2H_6, the

dx.doi.org/10.1021/jp310649n | J. Phys. Chem. B 2013, 117, 2153−2159

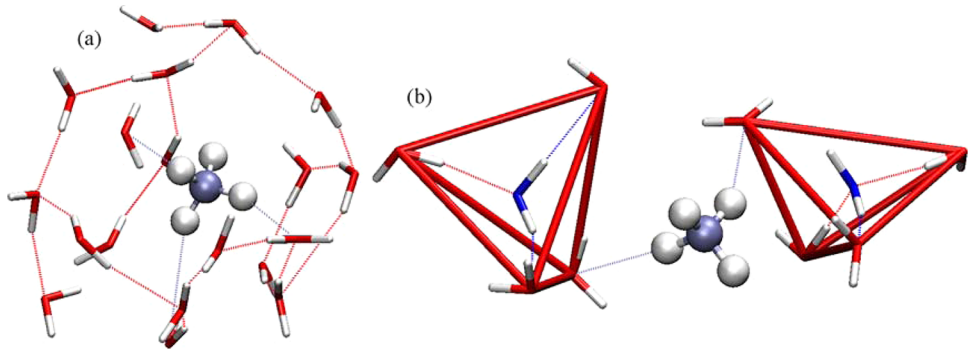

Figure 4. Snapshots of aqueous CH_4 showing (a) water's "cage" around methane, corresponding to the water molecules in the first hydration shell (R_1 and R_2), and (b) two water pentamers forming nearly perfect regular tetrahedra, with the central water molecule (in blue) in region R_2 and the water molecules at the four vertices (in red) in regions R_1, R_2, and R_3. The instantaneous q values were equal to (left) 0.900 and (right) 0.891 for these specific tetrahedra.

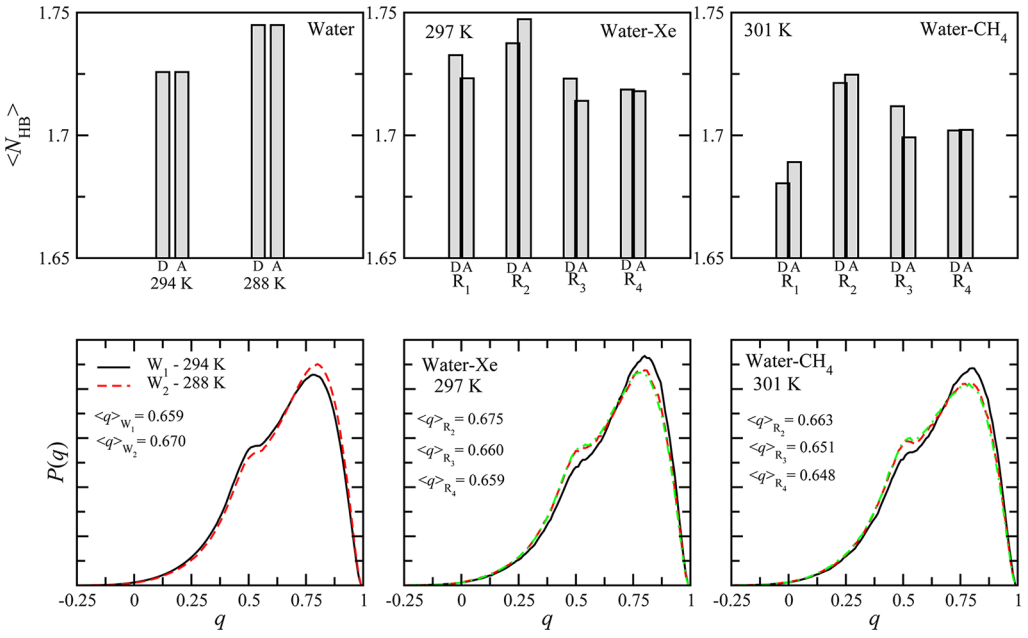

Figure 5. Average numbers of donor (D) and acceptor (A) H-bonds and tetrahedrality distribution in neat water and in the distinct regions around xenon and methane from MD (N,V,E) simulations. The average temperatures and pressures for neat water and for the xenon and methane solutions were [294 ± 4 K, −19 ± 717 atm], [288 ± 5 K, −72 ± 711 atm], [297 ± 5 K, −16 ± 709 atm], and [301 ± 5 K, −4 ± 712 atm], respectively.

tetrahedrality of water in R_2 is comparable to that of pure water at 283 K. This enhancement is much larger, for instance, than that recently reported for water in the second hydration shell of the halide anions in sodium halide aqueous solutions at low concentrations.[59]

Following our previous discussion on the distinction of R_1 and R_2, we recall that water molecules in R_1, especially for the hydrocarbons, often have the solute "substituting" for the fourth oxygen vertex, and therefore, the tetrahedrality of water molecules in R_1 is not directly comparable to that of neat water. Furthermore, even when a water molecule in R_1 is at the center of a water tetrahedron, this tetrahedron is distorted relative to those in bulk or neat water. This steric effect[30] is further related to the slower reorientational dynamics of water molecules near the solute, because the excluded volume of the solute cavity slows hydrogen-bond exchange.[38] Further, it should be noted that water molecules (O atoms) in R_1 are at the vertices of the tetrahedra with central water molecules in R_2 (see Figure 4b) and the tetrahedral enhancement observed in R_2 should be induced by the rearrangement of these small numbers (see caption of Figure 1) of water molecules nearest to the solute. The observed enhancement of the water tetrahedrality in R_2 is also consistent with recent results on the structure and energetics of hydrophobic hydration of a polypeptide.[60] The results of Matysiak et al.[60] indicate that apolar moieties of the polypeptide prevent the water molecules in the hydration shell from being approached by additional water molecules, which would lead to overcrowding and thus cause distortions among nearest-neighbor water molecules. Furthermore, the authors also observed that the water molecules in the hydrophobic hydration shell sample the hydrogen-bonding patterns present in comparable relatively low-coordination regions of bulk water. This picture is therefore also consistent with a moderate interpretation of the iceberg model where water molecules near hydrophobic groups and molecules adopt more tetrahedral arrangements and stronger H-bonds, also found in neat or bulk water at room temperature and more profuse in cold water.

Figure 4 shows water molecules in the first hydration shell (R_1 and R_2) forming a cage around methane (Figure 4a) and two water pentamers in which the central water molecules (in

dx.doi.org/10.1021/jp310649n | J. Phys. Chem. B 2013, 117, 2153−2159

blue) are in R_2 and the water molecules in the tetrahedron vertices (in red) belong to regions R_1−R_3. A smaller rearrangement should then occur for the next-nearest water neighbors (R_2), exerting a much weaker influence on the structure of water outside the first hydration layer. Notice that the tetrahedron vertices of the water molecules in R_3 belong to regions R_2−R_4. Hence, if a significant rearrangement occurred for those water molecules in R_2, a large tetrahedral ordering should propagate to R_3. For instance, for the methane solution, the average tetrahedrality of the water molecules in R_3 was already equal to 0.657, closer to the value of 0.651 for neat water and significantly lower than that in R_2, 0.673. The rearrangement of the H-bond network of water in R_1 is expected because water−water interactions are more favorable than solute−water interactions and this rearrangement permits water to minimize the number of broken H-bonds around the cavity where the solute is lodged. Thus, these results indicate that water around small nonpolar solutes has a more icelike structure, although not nearly like that sometimes associated with the iceberg model of Frank and Evans. The tetrahedral enhancement observed here is to be contrasted with the results from two-dimensional IR spectroscopy,[44] which "suggest that water molecules in the hydrophobic solvation shell do not exhibit an increased tetrahedral ordering compared with the bulk". Thus, our results restore, to some extent, the expected relationship between the structure and dynamics of the H-bond network of water, similar to a temperature effect, although, as discussed next, solute hydration effects cannot be exactly mapped onto the effects of temperature.

Before we discuss the radial distribution functions of water in hydrophobic solutions, we consider the structural results obtained from MD simulations in the microcanonical ensemble. Figure 5 shows the average numbers of H-bonds and the distribution of the tetrahedral parameter q for neat water and for the xenon and methane solutions. The MD (N,V,E) average temperature and pressure corresponding to the MD (N,P,T) simulations of neat water at 298 and 283 K were 294 ± 4 K and −19 ± 717 atm and 288 ± 5 K and −72 ± 711 atm, respectively, and for the xenon and methane solutions, the average temperatures and pressures were 297 ± 5 K and −16 ± 709 atm and 301 ± 5 K and −4 ± 712 atm, respectively. The H-bond donor and acceptor populations displayed in Figure 5 are very similar to those reported in Figure 2. For the tetrahedrality, although slightly different average values were found, a similar enhancement of the orientational order of water in region R_2 around the nonpolar solutes can be observed, although the tetrahedrality appears to be especially sensitive to temperature and pressure variations. For instance, the average values of q in the second hydration shells (R_3 and R_4) of xenon and methane are relatively different, although consistent with the lower average temperature of the xenon solution. Further, the tetrahedrality of water in R_2 of xenon is higher than that in neat water at 288 K and similar to the value found through MD (N,P,T), although the values in R_3 and R_4 are slightly larger. The solute−water partial radial distribution functions were found to be similar to those reported in Figure 1 and are omitted here. Thus, despite the observed differences, at least partially related to temperature and pressure differences, the thermostat and barostat of Berendsen et al. do not appear to affect the structure of water significantly, and increases in both the number of H-bonds and the tetrahedrality of water in R_2 of the hydrophobic solutes were observed when the trajectories were propagated in the micocanonical ensemble.

Water Radial Distribution Functions. Figure 6 shows the partial RDFs of pure water at 298 and 283 K and those for the methane aqueous solution. The latter are given for water molecules in R_2 and for all of the water molecules in the methane solution. Even though the tetrahedral orientational order of water in R_2 is comparable to the tetrahedrality of neat water at 283 K, the RDFs for water molecules in R_2 do not exhibit marked differences relative to the RDFs of water at 298 K. The water void occupied by methane lowers the height of the RDFs for distances larger than ∼3 Å, the onset of the CH_4−OW RDF (see Figure 1). Thus, comparison of the RDFs is restricted to the first (intermolecular) peak of the pair correlation functions. A small increase of the first peak is observed for the O−H partial RDF and, to a minor extent, the O−O partial RDF, whereas the first peak of the H−H RDF is shifted inward. Nevertheless, the positions of the maxima are almost unchanged, unlike in pure water at 283 K, relative to those in water at 298 K. The pair correlation functions computed for all of the water molecules in the methane solution, in turn, do not show any noticeable differences from those in pure water, consistent with experimental neutron diffraction results.[10] The situation is similar for Xe, C_2H_6, and C_6H_6, so these results are omitted here. Thus, the changes in the structure of a small subset of water molecules in the first hydration shell (R_2) of the hydrophobic solutes become imperceptible when the structure is averaged over all of the water molecules in the solution. This ensemble of water molecules, however, has a slightly larger number of H-bonds (see Figure 2), explaining the larger O−H coordination number in R_2. Further insight into the relationship between the water

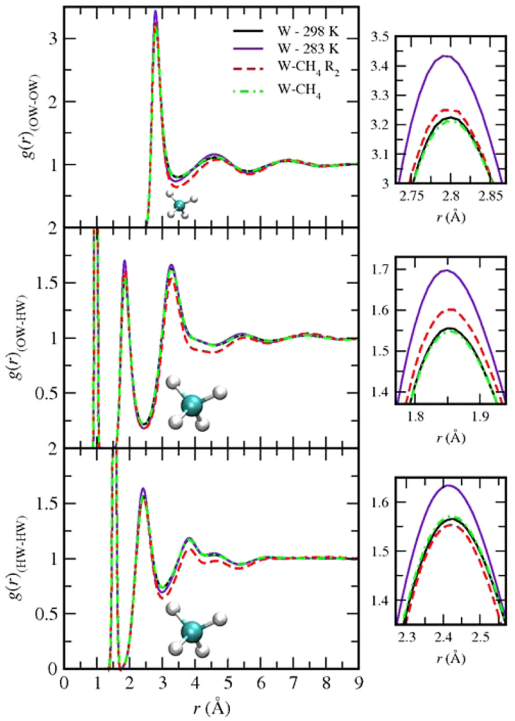

Figure 6. Water partial RDFs in neat water at 298 and 283 K and in methane aqueous solution at 298 K. The RDFs for the methane solution were computed for the water molecules in region R_2 (W−CH_4 R_2) and for all water molecules in the solution (W−CH_4). The void created by methane at ∼3 Å (onset of the CH_4−OW RDF) can be observed in the W−CH_4 R_2 water partial RDF.

dx.doi.org/10.1021/jp310649n | J. Phys. Chem. B 2013, 117, 2153−2159

structure in R_2 and that in liquid water at low temperatures can be obtained from the calculation of the local structure around a water molecule, avoiding differences in water number density. Thus, we computed the average distance of each O atom from the four nearest O atoms of neighbor water molecules, r_{O4}; the average distance of each O atom from the nearest two H atoms, r_{OH2}; and the average distance of each H atom from the nearest O atom, r_{HO1}. Figure 7 shows a small, although non-negligible,

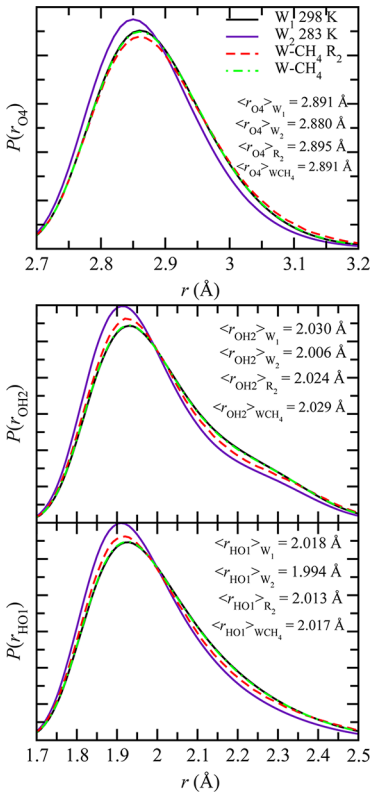

Figure 7. Distributions of the local distance parameters r_{O4}, r_{OH2}, and r_{HO1} for neat water at 298 and 283 K and in methane aqueous solution for water molecules in region R_2 and for all water molecules in the solution. The average values are given in the plots.

contraction of the r_{O4}, r_{OH2}, and r_{HO1} distances for water at 283 K, relative to those in pure water at 298 K. This is in contrast with the water molecules in R_2 of the methane solution, where a minimal expansion of r_{O4} and a contraction of r_{OH2} and r_{HO1} were observed. Thus, despite the similarity between the tetrahedral ordering for neat water at low temperatures and around hydrophobic solutes, the latter is not accompanied by a local compression. When averaging over all of the water molecules in the methane solution, these minor differences are no longer observable. The situation is similar for the other hydrocarbons and for xenon and methane, according to MD simulations in the microcanonical ensemble. For instance, for water at 294 and 288 K, from MD (N,V,E), the average value of r_{O4} is 2.888 and 2.885 Å, respectively, and for xenon and methane in R_2, the value is 2.894 and 2.895 Å, respectively. Thus, unlike in water at low temperatures, water molecules rearrange around small hydrophobic solutes without changing the O−O distance significantly. From this perspective, the water structure is largely preserved around small nonpolar solutes, consistent with the neutron diffraction results and with the general molecular picture of hydrophobic hydration.

The present results indicate, however, that water ordering around small hydrophobic solutes *does* contribute to the negative entropy and the large heat capacity that characterize the transfer of a nonpolar molecule to water, opposite to the current view on hydrophobic hydration.

CONCLUDING REMARKS

The local structure of water in the hydration shells of aqueous solutions of small hydrophobic molecules was studied through MD simulations and compared to that of neat water at 298 and 283 K. The results show that water rearranges around a hydrophobic solute in a more ordered way than in neat water and in the bulk, at room temperature, avoiding the enthalpic penalty associated with a significant loss of water−water H-bonds. Nevertheless, although we observed a significant tetrahedral enhancement of water in the first hydration shell, the enhancement was not larger than that observed for water at 10 °C, very different from ice, thus supporting a moderate view of the iceberg model of Frank and Evans. Further, this tetrahedral ordering is not associated with a contraction of the H-bond network, in particular a decrease of the O−O and O−H distances, characteristic of liquid water at low temperatures. Thus, instead we observed a minor increase and decrease of the O−O and O−H distances, respectively. Neither these differences nor the enhanced tetrahedrality can be inferred from the water partial radial distribution functions in hydrophobic solutions, which are nearly identical to those of neat water. This explains why this structural enhancement is not observed through neutron diffraction experiments. The tetrahedrality of water around hydrophobic solutes could, however, be probed "experimentally" through empirical potential structure refinement simulations.[10]

The water ordering discussed here should also occur around hydrophobic groups of more complex systems, and a similar analysis of the water structure should prove useful in understanding the thermodynamics of hydration of large amphiphilic molecules and molecular assemblies. The present results suggest, for instance, that the large heat capacity increase associated with the water exposure of hydrophobic amino acid residues on protein denaturation should be characterized by a significant ordering around the residues, decreasing the orientational entropy of water. Further, the relationship between the translational and reorientational dynamics of water near nonpolar molecules and groups and the tetrahedrality of water are of particular interest, in view of the recent controversy on the extent of the slowdown of the reorientational dynamics of water near hydrophobic groups, and is currently under investigation.

AUTHOR INFORMATION

Corresponding Author

*E-mail: ngalamba@cii.fc.ul.pt.

Notes

The authors declare no competing financial interest.

ACKNOWLEDGMENTS

The author gratefully acknowledges financial support from Fundação para a Ciência e a Tecnologia from Portugal through Project PTDC/QUI-QUI/113376/2009.

REFERENCES

(1) Blokzijl, W.; Engberts, J. *Angew. Chem., Int. Ed. Engl.* **1993**, *32*, 1545.
(2) Ball, P. *Chem. Rev.* **2008**, *108*, 74.
(3) Chandler, D. *Nature* **2005**, *437*, 640.
(4) Kauzmann, W. *Adv. Protein Chem.* **1959**, *14*, 1.
(5) Privalov, P. L.; Gill, S. J. *Adv. Protein Chem.* **1988**, *39*, 191.
(6) Southall, N. T.; Dill, K. A.; Haymet, A. D. J. *J. Phys. Chem. B* **2002**, *106*, 521.
(7) Frank, H. S.; Evans, M. W. *J. Chem. Phys.* **1945**, *13*, 507.
(8) Lipscomb, L. A.; Zhou, F. X.; Williams, L. D. *Biopolymers* **1996**, *38*, 177.
(9) Head-Gordon, T. *Proc. Natl. Acad. Sci. U.S.A.* **1995**, *92*, 8308.
(10) Buchanan, P.; Aldiwan, N.; Soper, A. K.; Creek, J. L.; Koh, C. A. *Chem. Phys. Lett.* **2005**, *415*, 89.
(11) Scatena, L. F.; Brown, M. G.; Richmond, G. L. *Science* **2001**, *292*, 908.
(12) Lum, K.; Chandler, D.; Weeks, J. D. *J. Phys. Chem. B* **1999**, *103*, 4570.
(13) Stillinger, F. H. *J. Solution Chem.* **1973**, *2*, 141.
(14) Chau, P. L.; Mancera, R. L. *Mol. Phys.* **1999**, *96*, 109.
(15) Graziano, G. *J. Chem. Soc., Faraday Trans.* **1998**, *94*, 3345.
(16) Lee, B. *Biopolymers* **1985**, *24*, 813.
(17) Lee, B. *Biopolymers* **1991**, *31*, 993.
(18) Lee, B.; Graziano, G. *J. Am. Chem. Soc.* **1996**, *118*, 5163.
(19) Lucas, M. *J. Phys. Chem.* **1976**, *80*, 359.
(20) Hummer, G.; Garde, S.; Garcia, A. E.; Paulaitis, M. E.; Pratt, L. R. *J. Phys. Chem. B* **1998**, *102*, 10469.
(21) Hummer, G.; Garde, S.; Garcia, A. E.; Pohorille, A.; Pratt, L. R. *Proc. Natl. Acad. Sci. U.S.A.* **1996**, *93*, 8951.
(22) Hummer, G.; Pratt, L. R.; Garcia, A. E. *J. Phys. Chem.* **1996**, *100*, 1206.
(23) Ashbaugh, H. S.; Truskett, T. M.; Debenedetti, P. G. *J. Chem. Phys.* **2002**, *116*, 2907.
(24) Ashbaugh, H. S.; Pratt, L. R. *Rev. Mod. Phys.* **2006**, *78*, 159.
(25) Gill, S. J.; Dec, S. F.; Olofsson, G.; Wadso, I. *J. Phys. Chem.* **1985**, *89*, 3758.
(26) Ben-Amotz, D.; Underwood, R. *Acc. Chem. Res.* **2008**, *41*, 957.
(27) Graziano, G.; Lee, B. *J. Phys. Chem. B* **2005**, *109*, 8103.
(28) Bakulin, A. A.; Pshenichnikov, M. S.; Bakker, H. J.; Petersen, C. *J. Phys. Chem. A* **2011**, *115*, 1821.
(29) Haselmeier, R.; Holz, M.; Marbach, W.; Weingaertner, H. *J. Phys. Chem.* **1995**, *99*, 2243.
(30) Rezus, Y. L. A.; Bakker, H. J. *Phys. Rev. Lett.* **2007**, *99*, 148301.
(31) Ishihara, Y.; Okouchi, S.; Uedaira, H. *J. Chem. Soc., Faraday Trans.* **1997**, *93*, 3337.
(32) Kaatze, U.; Gerke, H.; Pottel, R. *J. Phys. Chem.* **1986**, *90*, 5464.
(33) Okouchi, S.; Moto, T.; Ishihara, Y.; Numajiri, H.; Uedaira, H. *J. Chem. Soc., Faraday Trans.* **1996**, *92*, 1853.
(34) Shimizu, A.; Fumino, K.; Yukiyasu, K.; Taniguchi, Y. *J. Mol. Liq.* **2000**, *85*, 269.
(35) Wachter, W.; Buchner, R.; Hefter, G. *J. Phys. Chem. B* **2006**, *110*, 5147.
(36) Yoshida, K.; Ibuki, K.; Ueno, M. *J. Chem. Phys.* **1998**, *108*, 1360.
(37) Qvist, J.; Halle, B. *J. Am. Chem. Soc.* **2008**, *130*, 10345.
(38) Laage, D.; Stirnemann, G.; Hynes, J. T. *J. Phys. Chem. B* **2009**, *113*, 2428.
(39) Rossato, L.; Rossetto, F.; Silvestrelli, P. L. *J. Phys. Chem. B* **2012**, *116*, 4552.
(40) Rossky, P. J.; Karplus, M. *J. Am. Chem. Soc.* **1979**, *101*, 1913.
(41) Zichi, D. A.; Rossky, P. J. *J. Chem. Phys.* **1986**, *84*, 2814.
(42) Silvestrelli, P. L. *J. Phys. Chem. B* **2009**, *113*, 10728.
(43) Geiger, A.; Rahman, A.; Stillinger, F. H. *J. Chem. Phys.* **1979**, *70*, 263.
(44) Bakulin, A. A.; Liang, C.; Jansen, T. L.; Wiersma, D. A.; Bakker, H. J.; Pshenichnikov, M. S. *Acc. Chem. Res.* **2009**, *42*, 1229.
(45) Titantah, J. T.; Karttunen, M. *J. Am. Chem. Soc.* **2012**, *134*, 9362.
(46) Turner, J.; Soper, A. K. *J. Chem. Phys.* **1994**, *101*, 6116.
(47) Ren, P. Y.; Ponder, J. W. *J. Comput. Chem.* **2002**, *23*, 1497.
(48) Ren, P. Y.; Ponder, J. W. *J. Phys. Chem. B* **2003**, *107*, 5933.
(49) Ponder, J. W. *TINKER: Software Tools for Molecular Design 5.1*; Washington University School of Medicine: Saint Louis, MO, 2010.
(50) Berendsen, H. J. C.; Postma, J. P. M.; Vangunsteren, W. F.; Dinola, A.; Haak, J. R. *J. Chem. Phys.* **1984**, *81*, 3684.
(51) Desiraju, G. R. *Acc. Chem. Res.* **1996**, *29*, 441.
(52) Mateus, M. P. S.; Galamba, N.; Cabral, B. J. C.; Coutinho, K.; Canuto, S. *Chem. Phys. Lett.* **2011**, *506*, 183.
(53) Allesch, M.; Lightstone, F. C.; Schwegler, E.; Galli, G. *J. Chem. Phys.* **2008**, *128*, 014501.
(54) Allesch, M.; Schwegler, E.; Galli, G. *J. Phys. Chem. B* **2007**, *111*, 1081.
(55) Mateus, M. P. S.; Galamba, N.; Cabral, B. J. C. *J. Chem. Phys.* **2012**, *136*, 014507.
(56) Schravendijk, P.; van der Vegt, N. F. A. *J. Chem. Theory Comput.* **2005**, *1*, 643.
(57) Chau, P. L.; Hardwick, A. J. *Mol. Phys.* **1998**, *93*, 511.
(58) Errington, J. R.; Debenedetti, P. G. *Nature* **2001**, *409*, 318.
(59) Galamba, N. *J. Phys. Chem. B* **2012**, *116*, 5242.
(60) Matysiak, S.; Debenedetti, P. G.; Rossky, P. J. *J. Phys. Chem. B* **2011**, *115*, 14859.